

# 50 Years of the Radiological Research Accelerator Facility (RARAF)

Stephen A. Marino

*Radiological Research Accelerator Facility, Columbia University, Irvington, New York 10533*

---

Marino, S. A. 50 Years of the Radiological Research Accelerator Facility (RARAF). *Radiat. Res.* **187**, 413–423 (2017).

The Radiological Research Accelerator Facility (RARAF) is in its 50th year of operation. It was commissioned on April 1, 1967 as a collaboration between the Radiological Research Laboratory (RRL) of Columbia University, and members of the Medical Research Center of Brookhaven National Laboratory (BNL). It was initially funded as a user facility for radiobiology and radiological physics, concentrating on monoenergetic neutrons. Facilities for irradiation with MeV light charged particles were developed in the mid-1970s. In 1980 the facility was relocated to the Nevis Laboratories of Columbia University. RARAF now has seven beam lines, each having a dedicated irradiation facility: monoenergetic neutrons, charged particle track segments, two charged particle microbeams (one electrostatically focused to <1  $\mu\text{m}$ , one magnetically focused), a 4.5 keV soft X-ray microbeam, a neutron microbeam, and a facility that produces a neutron spectrum similar to that of the atomic bomb dropped at Hiroshima. Biology facilities are available on site within close proximity to the irradiation facilities, making the RARAF very user friendly. © 2017 by Radiation Research Society

---

## HISTORY

The Radiological Research Accelerator Facility (RARAF) was commissioned on April 1, 1967 as a joint enterprise between members of the Brookhaven National Laboratory (BNL) Medical Research Center and scientists from the Radiological Research Laboratory (RRL) of Columbia University. It was funded as a user facility for radiobiology and radiological physics by a grant from the Atomic Energy Commission (AEC) under the joint direction of Dr. Harold H. Rossi, the second Director of the RRL and Dr. Victor P. Bond, an Associate Director of BNL.

The Cosmotron at BNL was a synchrotron commissioned in 1952 that used a model D1 4 MV Van de Graaff accelerator manufactured by the High Voltage Engineering

Corp. in 1950 as the injector. After 14 years of operation the Cosmotron was decommissioned on December 31, 1966 and at the suggestion of Dr. Bond the Van de Graaff became the principal component of the new facility.

## RARAF AT BNL

The Columbia members of RARAF led by Facility Manager Leon J. Goodman were responsible for the development, design and operation of the facility as well as performance of biological irradiations and the required radiation dosimetry. The BNL members of RARAF under the direction of Dr. Clarence M. Turner performed a complete overhaul of the accelerator: it was converted from pulsed beam production to continuous beam operation; a new gradient column and acceleration tube were installed, increasing the terminal potential to 4.2 MV; and a new ion source was installed to provide high currents of hydrogen ions for neutron production.

The Cosmotron was still in place because it was activated, so the first irradiation areas – the Shielded Horizontal (SH) and Shielded Vertical (SV) beam Areas (T1H and T1V, shown in Fig. 1) were constructed in a corner of the part of the building that had been allotted to RARAF. These areas were surrounded by thick-shield-block walls and ceiling because of the neutron fields that would be produced in them. The Cosmotron was removed in 1969, allowing the second phase of RARAF to proceed. Four additional target areas were constructed: three in a lightly shield area with no roof, designated the Target (T) Area (Area 2), and one in a completely Unshielded (U) Area (Area 3).

Beam transport to these target areas was provided by a switching magnet installed in front of the accelerator that bent the ion beam left through angles of 15°, 30° and 45°. The 45° beam line serviced two target areas; the beam either was transported to the U Area or bent in opposite vertical directions by a pair of identical magnets to produce a horizontal beam (T4) on a grated platform in the T Area at an elevation about 12 feet above the floor of the building, providing a low-scatter environment (Fig. 2). A shielded room with a 250 kVp X-ray machine and an adjacent biology preparation room with temperature and humidity control were also constructed, as was a small biology lab for cell culture, providing ease of access for biology research-

<sup>1</sup> Address for correspondence: P.O. Box 21, Irvington, NY 10533; email address: sm14@columbia.edu.

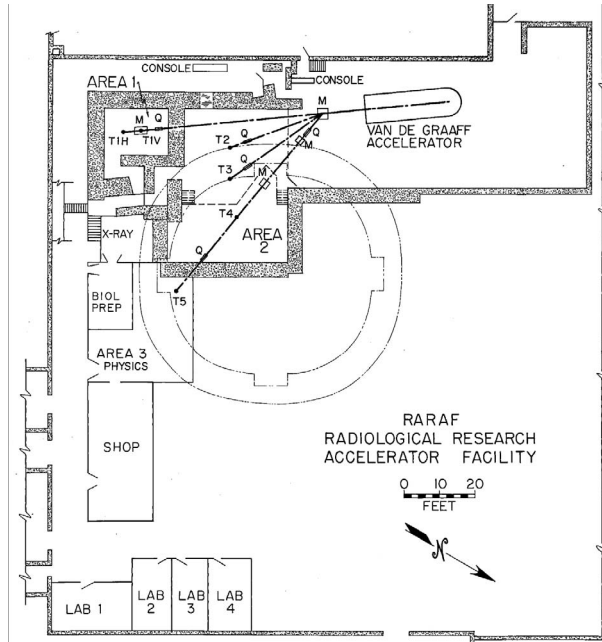


**FIG. 1.** The layout of RARAF at BNL in 1972. The SH and SV Areas target stations are labeled T1H and T1V, the elevated target station in the T Area (Area 2) is T4 and the U Area (Area 3) target station is T5. The Bio Prep and X-ray rooms are between Areas 3 and 1.

ers. By 1972 all target areas were functional. An elaborate redundant radiation safety system with sensors on doors, beam stops and valves designed by Leon Goodman and the Instrumentation Division (*I*) that had been partially installed in 1969 was completed.

#### *International Neutron Dosimetry Intercomparison*

In 1973 RARAF hosted the International Neutron Dosimetry Intercomparison (INDI). Thirteen groups from six countries (England, France, The Federal Republic of Germany, Japan, the Netherlands and U.S.) visited RARAF to perform mixed-field dosimetry on several neutron fields. Two or three groups visited for two weeks every other month and the RARAF group made measurements three times – once at the beginning, once in the middle and once at the end of the intercomparison. Measurements of neutron and gamma-ray kerma were made on beam line T4 for 0.67, 2.1, 5.5 and 15.1 MeV monoenergetic neutrons and for an intense  $^{252}\text{Cf}$  source. Measurements also were made in a water phantom for 5.5 and 15.1 MeV neutrons. The results obtained by the different groups were compared and analyzed in an ICRU Report 27 (2).

#### *RARAF Move*

BNL had been working on the development of the proton collider Isabelle and required additional space in the Cosmotron Building. To maintain RARAF, in 1978 the size of the facility was reduced, complete control was

transferred to BNL and Dr. Norman Rohrig of BNL became the Facility Manager.

The continued need for space for Isabelle forced RARAF to relocate in 1980. A search of available space at BNL revealed that there were no buildings that could be readily modified to house RARAF. Dr. Rossi was aware that the Columbia University cyclotron at Nevis Laboratories in Irvington, NY had been decommissioned in 1978 and was in the process of being dismantled. He negotiated with the Physics Department and obtained the south portion of the building, which the cyclotron had occupied (3). Nevis Laboratories is much closer to the RRL and is readily accessible by train.

The last day of accelerator operation at BNL was March 28, 1980. The entire RARAF facility was then dismantled and prepared for shipping.

#### **RARAF AT NEVIS LABORATORIES**

The move was completed before September 1, 1980. In 1981, control of RARAF was transferred back to the RRL and Dr. Paul Goldhagen became the Facility Manager.

The footprint at Nevis was smaller than at BNL so the design called for three floors on the north half of RARAF and two on the south half due to the high ceiling required in the accelerator area. The design of the new facility maintained the SH and SV Areas and the X-ray and biology preparation rooms essentially the same as they were at BNL, the T Area was greatly reduced in size and did not have a raised beamline and the U Area was enlarged (Fig. 3). The second floor included a biology lab three times the size of the one at BNL, a dish preparation lab and two other labs/offices. The 3rd floor was unfinished due to funding and was used as storage.

The directions of the beam lines had to be changed to accommodate the new geometry of the irradiation areas. Now the beam line to the SH/SV Areas is  $10.5^\circ$  right, the beam lines in the T Area are  $30^\circ$  and  $45^\circ$  right and the beam line to the U Area is  $50^\circ$  left.

The first irradiation was in March 1984, using the track segment facility. As at BNL, for the next five years the major use of RARAF was for irradiations using the monoenergetic neutron, track segment and molecular ion beam facilities.

#### *Changes in Leadership and Funding*

In 1985 Dr. Rossi stepped down as Director of the RRL and RARAF and Dr. Eric J. Hall became the third RRL Director and Director of RARAF. In 1989, Goldhagen left the CRR and Stephen A. Marino became the Facility Manager.

RARAF had been funded as a national facility by the AEC and its descendent departments: the Energy Research and Development Administration (ERDA) and then the Department of Energy (DOE). DOE funding terminated in

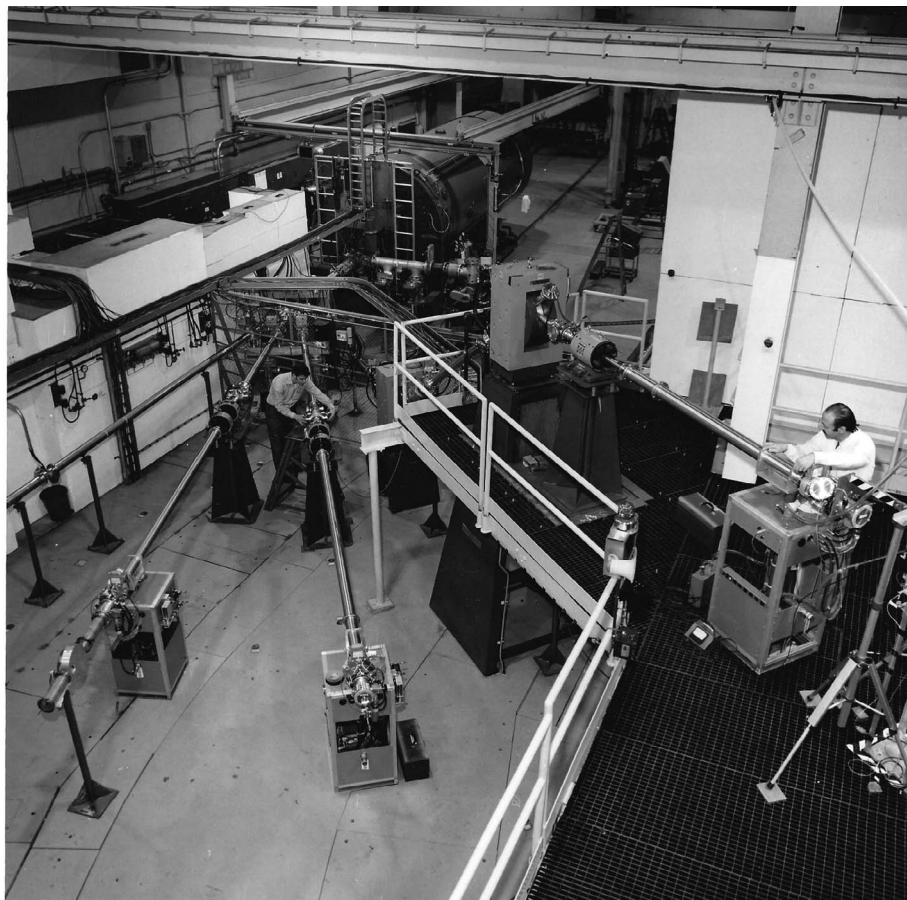


**FIG. 2.** A view of the T Area, including the 15°, 30° and elevated 45° beam lines. The Van de Graaff is visible at the top and the beamline to the SH/SV cave is along the left side. Leon Goodman is on the platform on the right. (Courtesy of Brookhaven National Laboratory)

1996. Dr. David J. Brenner of the Center for Radiological Research (CRR, former RRL) obtained funding for development of instrumentation and facilities from the National Center for Research Resources (NCRR) of NIH and took over the directorship of RARAF from Dr. Hall. In 2009 the grant was transferred to the National Institute of Biomedical Imaging and Bio-engineering (NIBIB).

#### *Accelerator Replacement*

Through the efforts of Dr. Brenner a high-end instrumentation grant was received from the NCRR in 2004 for a new accelerator. The existing Van de Graaff was then 54 years old; many replacement parts were no longer available; and a new accelerator would have much less energy spread in the beam, enabling the microbeam to focus to a smaller beam

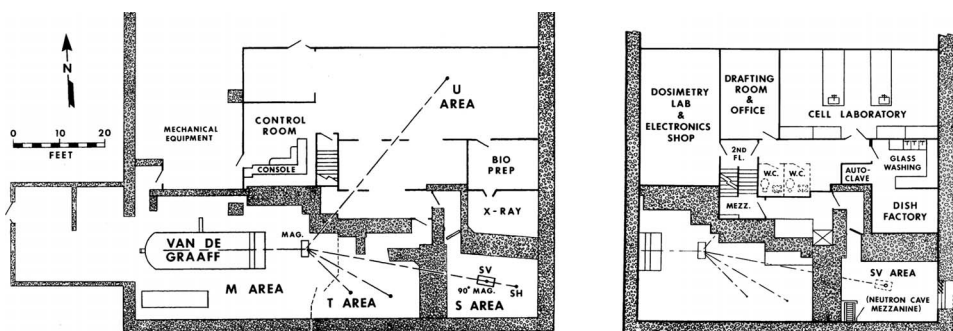


**FIG. 3.** Layout of the first (left) and second (right) floors of RARAF at Nevis Labs. Three of the beams are now bent to the right. Note the much smaller T Area and the shorter U Area beam line. The SH and SV Areas are essentially unchanged. An office and labs are on the second floor.

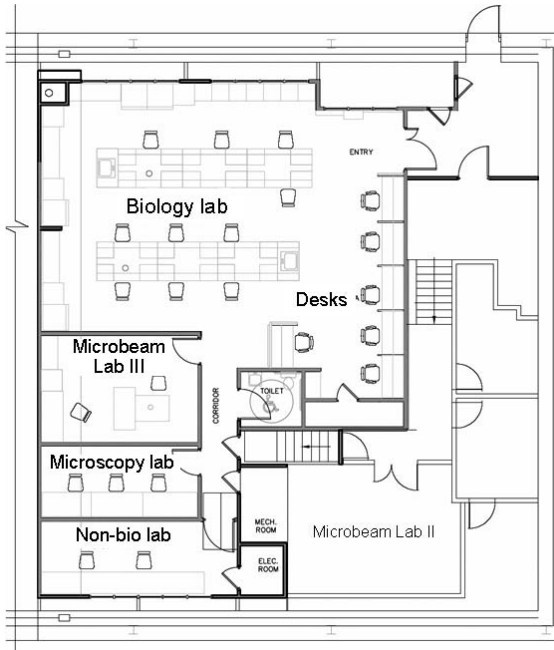


**FIG. 4.** The third-floor laboratories. There is office space on the right side of the Biology Lab. Microbeam III houses the PMM. Microbeam II and the other rooms on the right side are a half floor below the third floor.

spot size. A 5.5 MV Singletron from High Voltage Engineering Europa (HVE) was selected, not only because of the low voltage ripple ( $<100$  V at 3.75 MV) but also because, unlike a Van de Graaff or a Pelletron, there are no moving parts in the charging system. Large electrodes above and below the acceleration column induce charge on the column from a high-frequency high-voltage power supply.

June 11, 2005 was the last day the Van de Graaff was operated. By September 20th all the accelerator parts had arrived as had the technicians from HVE and assembly began. On December 2nd, the accelerator was completely assembled, tested and accepted – less than 6 months after the Van de Graaff was last used.

### 3rd Floor Laboratory

The Trustees of Columbia University donated the funds required to build over 2,000 square feet of laboratory and office space on the 3rd floor of RARAF (Fig. 4), including a microscopy laboratory and a laboratory for the Permanent Magnet Microbeam (PMM). Construction was completed by December 2006. This has provided much-needed office space and the expanded lab space has been extremely useful, particularly for the Microbeam Training Course or when there are a number of visiting biologists.

## IRRADIATION FACILITIES

While RARAF was at BNL, irradiation facilities were designed by various members of RARAF. Starting in 1990, the basic ideas for new irradiation facilities originated from Dr. Gerhard Randers-Pehrson, although they were often developed by other members of RARAF.

### Monoenergetic Neutrons

The first monoenergetic neutron irradiation was in February 1969 using a tritium target borrowed from the research Van de Graaff at BNL, which minimized neutron scatter and attenuation. Targets using the same physical design with a layer of titanium loaded with tritium or deuterium have been used at RARAF ever since. The use of tritium and deuterium as target materials and protons and deuterons as the incident particles makes possible the production of semi-monoenergetic neutrons with energies over much of the range from 0.2 to 15 MeV as well as two low-energy neutron spectra. As can be seen in Table 1, most neutron energies are obtained using the  $T(p,n)^3\text{He}$  reaction, dose rates are relatively low except at the two highest energies, and for most energies there is  $\leq 3\%$  gamma-ray dose.

While RARAF was at BNL Leon J. Goodman, Stephen A. Marino and Robert E. Mills designed the specialized irradiation fixtures required to position samples and performed the total dose and X-ray dosimetry.

**TABLE 1**  
**Typical Neutron Irradiation Parameters Used for Radiobiology**

Neutron energy (MeV) and spread ( $\pm\%$ )	Approximate maximum dose rate at 10 cm (Gy/h)	Gamma-ray dose (%)	Production reaction	Incident ion energy (MeV)
0.067 spectrum	0.01	4	$T(p,n)^3\text{He}$	1.3
0.11 spectrum	0.02	2	“	1.4
0.22 (25)	0.20	1	“	2.0
0.3 (15)	0.35	1	“	2.5
0.44 (14)	0.5	1	“	2.65
0.67 (14)	0.6	2	“	2.8
1.0 (11)	1.1	1	“	1.9
1.5 (10)	0.8	2	“	2.8
1.9 (4)	2.5	2	“	2.8
2.8 (5)	1.6	3	“	4.0
6.0 (6)	7.0	6	$D(d,n)^3\text{He}$	3.1
13–15 (1–4)	10.0	6	$T(d,n)^4\text{He}$	0.6 (d <sub>3</sub> )

**TABLE 2**  
**Charged-Particle Beams for Radiobiology**

Particle	Energy (MeV)	Mean LET (keV/mm)	LET spread (%)	Dose rate (Gy/s)
p	4.1	10	±0.6	0.001–4
d	3.7	20	±2.0	0.001–8
d	2.4	30	+4, –3	0.001–8
d	2.0	40	+9, –7	0.001–8
d	1.8	55	+20, –12	0.001–8
<sup>4</sup> He	9.8	70	±2.5	0.001–8
<sup>4</sup> He	7.3	90	+4, –3	0.002–8
<sup>4</sup> He	6.1	120	+8, –6	0.003–8
<sup>4</sup> He	5.6	150	+15, –10	0.004–8
<sup>4</sup> He	5.3	180	+23, –14	0.004–8

Neutrons remained one of the main irradiation modalities at RARAF until the late 1990s, when demand for biological irradiations with monoenergetic neutrons declined significantly. Many different biological systems have been irradiated including bean and onion roots, *Tradescantia* flower buds, fruit flies, mammalian cells, mice and rats observing effects such as root growth, cell survival (4), mutations (5), micronuclei, chromosomal aberrations (6), oncogenic transformation (7), lens opacification, and leukemia and tumor production (8).

In addition to neutron microdosimetry, physics experiments have included, e.g., irradiation of thermoluminescent detectors (TLDs), fluorescent neutron track detectors (FNTDs) (9), track etch materials, liquid drop detectors (10), neutron spectrometers for use in space (11), and a liquid xenon detector used to search for weakly interacting massive particles (WIMPs).

#### *Molecular Ion Beam Experiment*

Dr. Rossi initiated an experiment in 1974 to determine the interaction between “sublesions” created by independent traversals of a cell nucleus by charged particles (12) - the “molecular ion beam experiment”. Development of this facility was accomplished by Robert Colvett of the RRL and Dr. Norman Rohrig of BNL.

Cells plated on a thin mylar surface glued to a steel ring were placed in a sealed fixture which was inserted into the accelerator vacuum system and maintained at a reduced atmosphere to avoid rupture of the mylar. The cells were irradiated with molecular ions that dissociated in the mylar, underwent multiple scattering and entered the cells simultaneously with mean separations from 90 to 800 nm, which were a function of the particle type and energy and the thickness of the mylar. The biological effects were compared to irradiations using single, uncorrelated ions of the same energy. A “zero” separation irradiation was obtained using <sup>3</sup>He ions with a linear energy transfer (LET) equal to the sum for the individual pairs or triads of ions.

Measurements of the scattering distributions for protons and deuterons were made (13) and used to determine the separation distributions of the ions. Analysis of the results of the experiment (14) indicated that the interaction between

sublesions primarily occurred at distances much less than a micron, one of the reasons for the advent of nanodosimetry. This system was replaced in 1983 with a similar system with cell dishes that had a much smaller diameter and therefore did not require the cells to be at reduced atmospheric pressure.

#### *Track Segment Facility*

In 1976 the “track segment” facility was developed by Colvett and Rohrig to irradiate cell monolayers with charged particles having a narrowly defined LET (15). The ion beam is defocused, passes through a slit-shaped collimator, exits the vacuum system through a thin metallic window and penetrates thin samples plated on dishes with 6- $\mu$ m thick mylar surfaces. The dishes are rotated across the beam for uniformity. By varying the ion energy and type LETs from 10 to 180 keV/ $\mu$ m can be achieved with a wide range of dose rates (Table 2).

Three dosimeters are used: a proportional counter to determine the average LET, an ion chamber to measure the dose rate and a solid-state detector that is movable to determine dose uniformity along the length of the beam. A 50 kV X-ray head is attached to the beam line to provide a comparison or standardization radiation.

This facility is very versatile. It has been in use essentially without modification since its initial construction and continues to be used frequently even today. In addition to cell cultures (16), the facility has been used to irradiate spores, thin layers of DNA in solution (17), 3D artificial tissue (18), TLDs (19), track etch dosimeters, and microchips. One result of irradiations using this facility was the measurement of oncogenic cell transformation as a function of LET (20, 21).

Although the ions are delivered randomly, the facility is used for some of the “bystander” irradiations in which only a fraction of the cells are irradiated and the effect on unirradiated cells is examined (22). A dish with narrow strips of mylar 38  $\mu$ m thick is inserted into a standard cell dish and cells are plated on the combination. Cells on the 6- $\mu$ m thick surface are irradiated with <sup>4</sup>He ions; those on the thick mylar are unirradiated since the total mylar thickness exceeds the range of the ions. This is particularly useful for low-yield

experiments that require many more cells than can be readily irradiated with the microbeam.

#### *Ultra-Low Energy X-Ray Facility*

In 1990 an ultra-low energy X-ray irradiation system was developed by Randers-Pehrson based on proton-induced X-ray emission (PIXE) using a gas cell with a thin metallic foil proton beam entrance window and a long, narrow X-ray exit opening. Characteristic  $K_{\alpha}$  X rays of carbon (277 eV, from  $\text{CH}_4$ ), neon (847 eV) and argon (2.96 keV) were produced. Cell dishes were rotated across the exit window to provide a uniform irradiation. Dose rates achieved were 3, 7 and 90 Gy/h for carbon, neon and argon, respectively.

#### *Collimated Charged Particle Microbeam*

By 1990 there was considerable interest in the effects of radon alpha particles. Exposures to the general public were normally so low that any lung cell would rarely be traversed by more than one alpha particle in its lifetime. This provided impetus for the development by Randers-Pehrson of a collimated single-particle microbeam. Design work on a collimated microbeam actually had begun in 1973 by Colvett but was interrupted by development of the Molecular Ion Beam and then the RARAF move.

A vertical beam was required but the SV Area was needed for the track segment facility. The office on the second floor was modified so that half the room would be a biology lab while the other half would be used for the irradiation facility (Microbeam I).

The two then-unused magnets that provided the elevated beam in the T Area at BNL were available (neither of which could bend the beam  $90^\circ$ ) and using the same bending angle only a single existing power supply would be required. The first magnet bent the beam  $70^\circ$  toward the lab and was tilted at a vertical angle of  $20^\circ$  so that the second magnet made the beam vertical, passing to the lab above through a hole in the floor.

Final collimation was provided by a  $5\text{-}\mu\text{m}$  diameter collimator followed  $300\ \mu\text{m}$  after by a  $6\text{-}\mu\text{m}$  anti-scatter collimator (23). This provided a main beam ( $\sim 92\%$ )  $6\ \mu\text{m}$  in diameter with a "penumbra" ( $\sim 7\%$ )  $8\ \mu\text{m}$  in diameter due to particles scattered by the first collimator that were transmitted through the second collimator. The particle beam diameter was determined by scanning a piece of thin material across the beam in orthogonal directions and observing the fraction of the beam that lost energy in the material. This method is also used for the electrostatically focused and permanent magnet microbeams described below.

A vibration isolation table, high-speed computer-controlled stage with  $0.2\ \mu\text{m}$  resolution, fluorescence microscope, light source, CCD television camera, computer and image analysis software were purchased in 1991 to create an end station. These items are the basis for all the microbeam end stations, although there are variations in the details.

The irradiation protocol developed for this microbeam is used for all the microbeams at RARAF. Cells are plated in a 3-mm diameter region on  $3\text{-}\mu\text{m}$  thick polypropylene glued over a hole in a standard plastic bacterial culture dish and their nuclei are stained with 50 nm Hoechst fluorescent dye. The dishes are scanned under computer control with a low-power objective to identify areas containing nuclei. Each of these areas is then scanned with a high-power objective to verify the positions of the nuclei with greater resolution just prior to irradiation of the cells in the image. A gas detector with an optically clear mica end window mounted around the high-power microscope objective is used to count the particles. Because the detector is after the sample and the ions have a very short range, essentially all the medium is removed from the cell dish before irradiation and humidified air/ $\text{CO}_2$  is supplied to maintain the cells.

Initially the irradiations were performed manually by positioning cell nuclei, observed by their fluorescence, to the beam location using a joy stick, a very labor-intensive method. Over the next several years the system was continually improved. Periodic replacements were made of the computers, image processor boards and imaging software, increasing the speed of the system. Irradiations are now under computer control, reducing strain on the operators and greatly increasing the irradiation rate to  $\sim 5,000$  cells/h.

New imaging software provided higher resolution images and additional image processing options, such as background subtraction, correction for nonuniform lighting and piecing together multiple initial scan images into a single, large image. A fast method to irradiate the cytoplasm of cells, rather than their nuclei, under computer control was developed. Cells are irradiated along the major axis of the nucleus at a fixed distance from the edge of the nucleus.

The collimated microbeam was used to demonstrate a reduced incidence of oncogenic transformation in C3H10T1/2 cells by a single alpha-particle traversal in a cell nucleus relative to a Poisson distribution of an average of one traversal from a broad beam (track segment facility) irradiation (24). Other experiments investigated mutagenesis due to an exact number of alpha particles in a cell nucleus (25), cytoplasmic irradiation (26) and the bystander effect (27).

#### *Electrostatically Focused Charged Particle Microbeam*

The size of the microbeam could not be decreased using collimation due to the rapid relative increase in scattering on the walls of the collimators as their diameters are reduced, so design of a focused microbeam began. Electrostatic quadrupole focusing was selected for several reasons: electrostatic lenses do not have the hysteresis inherent in magnetic lenses, stable voltage is more easily obtained than stable current, and the field strength required for focusing is independent of particle mass and charge for a given potential of the accelerator.

**TABLE 3**  
**Microbeam Beam Spot Development**

Year	Beam spot diameter ( $\mu\text{m}$ )	Microbeam system
1984	8	Collimated
2001	5	Single quadrupole quadruplet
2005	3.5	Single quadrupole triplet
2007	1.5	Double quadrupole triplet
2008	0.8	Double quadrupole triplet

The quadrupole quadruplet design by Randers-Pehrson and Dr. Alexander D. Dymnikov (28) consists of four ceramic rods with a thin coating of gold in bands forming the quadrupole elements on each rod. The insulating sections between the bands are the uncoated ceramic surfaces. The lengths of the elements are in proportion to the relative strengths required for focusing so that the voltages required on all elements are essentially the same to minimize the chances of sparking. The rods are clamped together in three places with v-blocks and separated by precision cross spacers with holes in their centers for beam transmission.

The initial quadrupole quadruplet lens was constructed in 1999 in the RRL shop. “Russian” symmetry was used (potentials  $+A$ ,  $-B$ ,  $+B$ ,  $-A$ ) to produce a circular beam spot of minimum size (Table 3).

Optics calculations for the design of a quadrupole system to focus the beam to submicron size determined that two quadrupole triplets with Russian symmetry (potentials  $+A$ ,

$-B$ ,  $+C$ ,  $-C$ ,  $+B$ ,  $-A$ ) would be required. To achieve this beam, space for the two quadruplet triplets and a much longer distance between the object aperture and the focal point were required, which could not be achieved in Microbeam I. The area on the floor above the exit of the Van de Graaff was selected for a new microbeam lab (Microbeam II). It had several advantages: the beam exit would be much further from the bending magnet; only a single  $90^\circ$  bend was required instead of a  $50^\circ$  bend and two  $70^\circ$  bends, simplifying transmission; and the floor was concrete, 27 inches thick, much more stable than the sheet metal beams in Microbeam I.

By June 2001, a  $90^\circ$  bending magnet had been installed and construction of Microbeam II was complete. The room had the same general layout as Microbeam I with half the room set up as a biology laboratory. A new end station was constructed (Fig. 5). The stage has nanometer resolution and 100  $\mu\text{m}$  z-axis motion but only a 200  $\mu\text{m}$  range in the x and y directions and is embedded in a coarser stage constructed in our shop to extend the x-y range to 1 cm. A silicon nitride window 500 nm thick is normally used as the exit window; a 100- $\mu\text{m}$  thick window, which is much more delicate, is used to minimize scatter when the smallest diameter beam is required.

The first double triplet was installed at the end of 2006. The two triplets were positioned in a long metal tube and aligned in our shop before the tube was placed in the beamline. In 2008 the compound lens was able to focus the

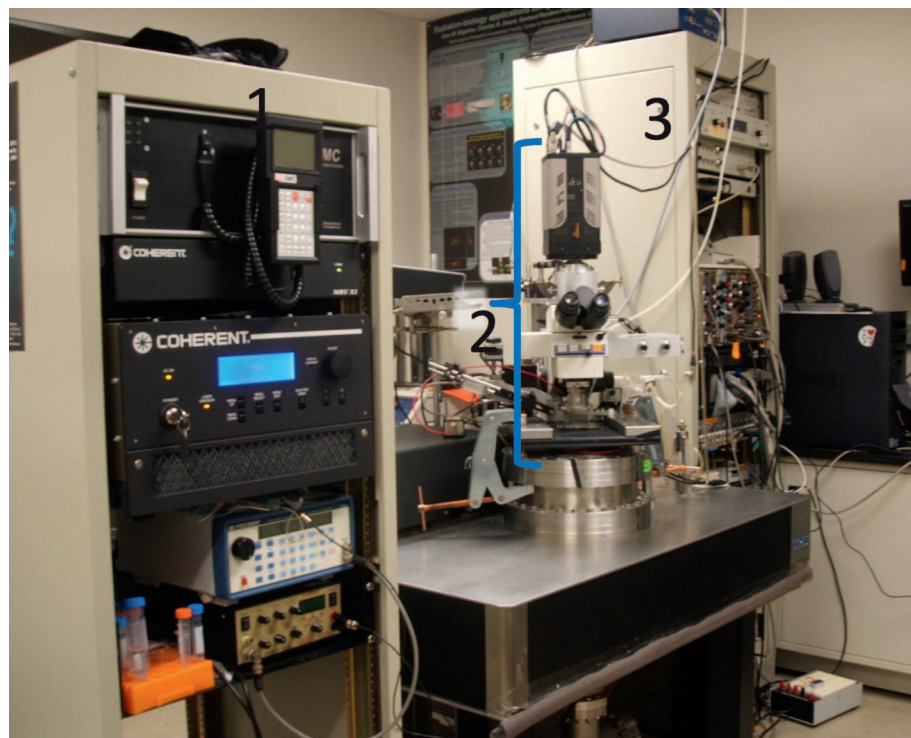


**FIG. 5.** The electrostatically focused single-particle microbeam facility in the new microbeam laboratory (Microbeam II): 1. The control electronics for the multiphoton laser; 2. the microbeam stage, microscope and camera; 3. the electronics rack containing instrumentation for the microbeam.



$^4\text{He}$  beam to  $0.8\ \mu\text{m}$  – a *submicron beam* (29). One of our collaborators (David Chen) developed a human HT1080 fibrosarcoma cell line in which the cells have been transfected with a XRCC1 DNA single-strand break repair protein tagged with green fluorescent protein. The microbeam was used to irradiate a specific pattern of locations in a single cell nucleus causing damage foci. The observed fluorescence of the foci was in the shape of the letters “NIH”, demonstrating the targeting capability of the microbeam.

The microbeam is presently undergoing additional development with the addition of a superconducting solenoid magnet to reduce the beam spot size to  $100\ \text{nm}$ . Stimulated emission depletion (STED) fluorescent microscopy is being developed to allow imaging at this resolution, enabling targeting of individual chromosomes.

In addition to the irradiation of cell nuclei and cytoplasm and cell bystander experiments (30), as were performed using the collimated microbeam, the electrostatically focused microbeam has been used to investigate the bystander effect in artificial tissue (31) and *C. elegans* worms (32). Irradiation of the ears of hairless mice demonstrated a bystander effect in a live mammalian system (33).

#### *Permanent Magnet Microbeam*

Development of a microbeam using permanent magnets began in 2004 by Dr. Guy Garty. The design was the same as for the electrostatically focused microbeam: two quadrupole triplets (34, 35). The strengths of the permanent magnets themselves are fixed; adjustments in quadrupole field strength are made by moving magnets slightly in or out relative to the quadrupole center.

Originally the helium ions were to be supplied by a  $^{210}\text{Po}$  source, which would have created a stand-alone microbeam that could be used when the accelerator was unavailable and be duplicated in facilities lacking an accelerator; however it became very difficult to obtain the isotope after the poisoning incident in London and the Singletron is used as the source of ions.

Since the original microbeam facility was no longer in use, the end station was moved to a lab directly above (Microbeam III) to have sufficient space for the two quadrupoles. The beam line was extended from the old collimated microbeam through the Microbeam I lab to the end station on the 3rd floor.

A beam spot  $20\ \mu\text{m}$  in diameter was obtained for  $^4\text{He}$  ions before the end station had to be disassembled for the 3rd floor construction (see below). After reassembly a year later and optical alignment of the beam line, this same spot size was achieved without tuning any of the magnets, demonstrating the stability of the system. After additional tuning the  $^4\text{He}$  beam was focused to  $5\ \mu\text{m}$ , the original goal in 2007. This permanent magnet microbeam (PMM) system is used for biological irradiations when the electrostatically

focused microbeam is unavailable and for any development project that would interfere with use of the other particle microbeam.

One particular project was the development of the Flow and ShooT (FAST) system (36) by Garty to irradiate the nuclei of cells flowing in a microfluidic channel. A split-coil magnet was installed near end of the beam line to deflect the particle beam to a given location. The beam position was mapped as a function of the magnet current required in each of the independent coils and shown to be linear in both the x and y directions. When the system was completed in 2013 a flow rate of  $500\ \text{mm/s}$  and  $\sim 10,000\ \text{cells/h}$  had been achieved with the targeted position within  $\pm 1.5\ \mu\text{m}$  of the true position 95% of the time.

#### *X-Ray Microbeam*

Design of a soft X-ray microbeam using PIXE (37) started in early 2005 and was developed by Dr. Andrew D. Harken. Unlike electrons, protons generate relatively no bremsstrahlung and therefore an essentially monoenergetic X-ray beam is produced.

A  $1.8\ \text{MeV}$  proton beam in the  $50^\circ$  beam line is focused by an electrostatic quadrupole quadruplet into an elliptical spot on a titanium target ( $4.5\ \text{keV K}_\alpha$  X rays) with an angled surface, which is embedded in a copper rod for cooling. X rays emitted in the vertical direction are focused using a  $120\text{-}\mu\text{m}$  diameter zone plate to a  $5\ \mu\text{m}$  diameter beam spot determined, as for the charged particle microbeams, by scanning a thin piece of material across the beam in orthogonal directions; however, in this case the amount of transmitted beam is measured.

The area between the beryllium vacuum window that transmits the X-ray beam and the X-ray focal point is filled with helium to minimize X-ray absorption. A beam current  $>2\ \mu\text{A}$  on the target yields an X-ray dose rate of  $>10\ \text{mGy/s}$ .

#### *Multiphoton Microscope and Microspot*

A multiphoton imaging system was developed in 2006 by Dr. Alan W. Bigelow. When the photon density is sufficiently high, two photons act as a single photon with half the wavelength (twice the energy). This allows a long wavelength to penetrate several hundred microns into tissue, producing little damage, while activating a fluorescent material in a small volume at the focal point.

A high-power tunable titanium sapphire laser with a wavelength range from  $680$  to  $1080\ \text{nm}$  is installed on the isolation table of the Microbeam II. The laser light is guided by a series of mirrors to a galvanometer scanning head used to raster the laser beam across the field of view of the microscope. The fluorescent emission is routed to two phototubes to provide simultaneous 2-color imaging (38). The system can produce 3D images by taking successive sections of a sample using the z-motion of the microbeam stage. The system can observe autofluorescence and second harmonic generation to avoid the addition of fluorophores.



The multiphoton system has been used to image *C. elegans* worms, artificial human umbilical vein structure, the hearts of zebrafish embryos and even mitochondria.

At sufficient power the beam spot (FWHM  $\sim 0.4 \mu\text{m}$  D,  $\sim 4 \mu\text{m}$  long) of the multiphoton system can induce single-strand breaks in DNA and can be used as an irradiation modality of its own (39). In a demonstration of the precision of the microspot, a single XRCC1 cell nucleus was irradiated in a pattern such that the fluorescence formed a detailed image of the Columbia University crown logo. Examples of microspot use are the creation of damage to specific cells in zebrafish embryo hearts and photobleaching mitochondria.

#### *Neutron Microbeam*

In 2009 Dr. Yanping Xu and Stephen Marino began development on the  $30^\circ$  beam line of a neutron microbeam, which is particularly difficult since neutrons have no charge and therefore cannot be focused and neutron collimation is limited to much larger beams. Near the threshold for the  ${}^7\text{Li}(p,n){}^7\text{Be}$  reaction at 1.881 MeV low-energy neutrons ( $<60 \text{ keV}$ ) are emitted in a very narrow forward angular distribution. At the back of a very thin lithium target, the diameter of this cone can be tens of microns (40).

A quadrupole quadruplet focuses the 1.886 MeV proton beam onto a gold foil  $20 \mu\text{m}$  thick with a  $1\text{-}\mu\text{m}$  thick coating of  ${}^7\text{LiF}$ . In 2013 the proton beam was focused to a  $10 \mu\text{m}$  diameter and a  $36 \mu\text{m}$  diameter neutron beam was measured - the *first neutron microbeam in the world*.

The neutron beam diameter was measured using an FNTD with a thin  $\text{Li}^6\text{F}$  layer. The ions produced by the  ${}^6\text{Li}(n,\alpha){}^3\text{H}$  reaction, particularly the  ${}^3\text{H}$  ions, produce tracks in the FNTD that can be visualized using a laser, allowing indirect determination of the neutron beam diameter.

The neutron dose rate provided by the  $10 \text{ nA}$  proton current is estimated to be  $270 \text{ mGy/min}$ . Instrumentation to measure the neutron fluence and perform biological irradiations is still under development.

#### *Hiroshima Neutron Spectrum*

Development was begun in 2011 by Xu and Marino of a new fast neutron source with a broad energy spectrum which extends to  $10 \text{ MeV}$  and emulates that of the “Little Boy” atomic bomb at Hiroshima  $1.5 \text{ km}$  from ground zero (41). A mixed beam of  $5 \text{ MeV}$  monatomic, diatomic and triatomic protons and deuterons is incident on a thick beryllium target producing neutrons from the  ${}^9\text{Be}(d,n){}^{10}\text{B}$  and  ${}^9\text{Be}(p,n){}^9\text{B}$  reactions. The diatomic and triatomic particles break up on contact with the target into individual ions with  $2.5$  and  $1.67 \text{ MeV}$  energies, respectively, enhancing the lower-energy portion of the spectrum. To produce this mixed beam a gas source with a ratio of hydrogen to deuterium of  $1:2$  is used in the Singletron ion source. A new  $0^\circ$  beam line was constructed which requires no deflection of the particle beam; therefore there is no

separation of different ions and the full beam from the accelerator is utilized.

Neutron spectroscopy was performed and verified that the neutron spectrum created is a close match to that at Hiroshima. The neutron dose rate is  $0.13 \text{ Gy/h}/\mu\text{A}$ , allowing doses of  $1 \text{ Gy}$  to be delivered in  $<1 \text{ h}$ , and the gamma-ray dose rate is  $\sim 17\%$  of the total dose rate. Mice and human blood samples are placed in tubes and mounted on a “Ferris wheel” that rotates around the target to average out variations in dose rate around the target and to create a multi-lateral irradiation.

### DISSEMINATION AND TRAINING

In addition to the research performed at RARAF and publications in journals, staff members disseminate information through meetings as well as train post-doctoral fellows and researchers in microbeam development and use. They also have trained high school, undergraduate and graduate students in various aspects of radiobiology and radiological physics.

#### *International Microbeam Workshops*

In 1997 RARAF hosted at Columbia University the 3rd International Workshop: Microbeam Probes of Cellular Radiation Response. This biannual 2-3-day workshop brings together groups interested in developing and applying micro-irradiation techniques to study cell and tissue damage and subsequent biological response. Over the years, participation has grown from  $<50$  to  $100$  or more participants. RARAF has hosted this workshop three additional times since 1997: the 4th Workshop in 1999 in Dublin, Ireland and the 7th and 10th workshops, 2006 and 2012, at Columbia University.

#### *Microbeam Training Course*

A microbeam training course “Single-Cell Microbeams: Theory and Practice” was initiated in 2011 and has been given annually except in 2015 (42). This three-day course consists of lectures, demonstrations and hands-on experience and is limited to  $6\text{--}8$  participants to enhance its intimate nature. The course is designed to cover the specifics of microbeam theory and practice for biological research (e.g., imaging, designing a microbeam facility).

### SUMMARY

For 50 years RARAF has provided irradiation facilities and precision dosimetry for biologists and physicists from the United States and other countries. Approximately 400 publications, including at least 15 Master’s and Ph.D. theses, have resulted from data obtained, at least in part, at RARAF. More than 100 undergraduate and graduate students, post-doctoral fellows, and researchers have received training, many of whom were from China,

Germany and Japan. Several have become full professors with their own laboratories and one is even director of an accelerator facility with a charged particle microbeam.

RARAF now has seven beam lines, each providing a dedicated irradiation facility: monoenergetic neutrons, charged particle track segments, two charged particle microbeams (one electrostatically focused to  $<1 \mu\text{m}$ , one magnetically focused), a soft X-ray microbeam, a neutron microbeam and a facility that produces a broad neutron spectrum similar to that of the atomic bomb dropped at Hiroshima. Biology facilities are available within one to a few meters, making the RARAF very user friendly. Additional information and a full publication list can be found at RARAF.org.

### ACKNOWLEDGMENTS

RARAF has existed for 50 years due to the efforts of the many scientists, technicians, machinists and others who contributed to its design, development and operation. We would particularly like to thank: Rudolph Gand of the RRL and especially Gary W. Johnson of the CRR for the design and construction of many of the instruments and fixtures used at RARAF; Dr. Charles R. Geard for his encouragement to develop a charged particle microbeam, for all the biological expertise he has contributed, and for assistance with this manuscript; and RARAF biologists Drs. Brian Ponnaiya and Manuela Buonanno for assistance in developing biological irradiation fixtures and protocols. During its lifetime RARAF has been supported by the Atomic Energy Commission (AEC), the Energy Research and Development Agency (ERDA), the Department of Energy (DOE), the National Center for Research Resources (NCRR) of the National Institutes of Health (NIH), and finally by the National Institute of Biomedical Imaging and Bio-engineering (NIBIB) of NIH.

Accepted: January 15, 2017; published online: January 31, 2017

### REFERENCES

- Hartin WJ, Goodman LJ. An improved safety system. *Health Phys* 1971; 20:73–81.
- An International Neutron Dosimetry Intercomparison. ICRU Report 27. Washington, D.C.: International Congress on Radiation Units and Measurements; 1978.
- Rossi HH. The Radiological Research Accelerator Facility at Columbia University. *Nucl Inst Meth B* 1985; 10/11:1086–89.
- Hall EJ, Novak JK, Kellerer AM, Rossi HH, Marino S, Goodman LJ. RBE as a function of neutron energy. I. Experimental observations. *Radiat Res* 1975; 64:245–55.
- Sparrow AH, Underbrink, AG, Rossi HH. Mutations induced in *Tradescantia* by small doses of x rays and neutrons: Analysis of dose-response curves. *Science* 1972; 176:916–8.
- Pandita TK, Geard CR. Chromosome aberrations in human fibroblasts induced by monoenergetic neutrons. I. Relative biological effectiveness. *Radiat Res* 1996; 145:730–9.
- Miller RC, Geard CR, Brenner DJ, Komatsu K, Marino SA, Hall EJ. Neutron-energy-dependent oncogenic transformation of C3H 10T1/2 mouse cells. *Radiat Res* 1989; 117:114–27.
- Shellabarger CJ, Brown RD, Rao AR, Shanley JP, Bond VP, Kellerer AM, et al. Rat mammary carcinogenesis following neutron or x-radiation. In: *Biological Effects of Neutron Irradiation*. Vienna: IAEA; 1974. p. 391–401.
- Sykora GJ, Akselrod MS, Salasky M, Marino SA. Novel  $\text{Al}_2\text{O}_3:\text{C,Mg}$  fluorescent nuclear track detectors for passive neutron dosimetry. *Radiat Prot Dosim* 2007; 126:278–83.
- Apfel RE. Characterization of new passive superheated drop (bubble) dosimeters. *Radiat Prot Dosim* 1992; 44:343–6.
- Kinnison JD, Maurer RH, Roth DR, Haight RC. High energy neutron spectroscopy with thick silicon detectors. *Radiat Res* 2003; 159:154–60.
- Rossi H.H. Biophysical studies with spatially correlated ions: 1. Background and theoretical considerations. *Radiat Res* 1979; 78:185–91.
- Colvett RD, Rohrig N. Biophysical studies with spatially correlated ions: 2. Multiple scattering, experimental facility, and dosimetry. *Radiat Res* 1979; 78:192–209.
- Kellerer AM, Lam Y-MP, Rossi HH. Biophysical studies with spatially correlated ions: 4. Analysis of cell survival data for diatomic deuterium. *Radiat Res* 1980; 83:511–28.
- Rohrig N, Colvett RD. Charged-particle beams for radiobiology at RARAF. In: *Annual Report on Research Project, ERDA report COO-3243-5*. Springfield, VA: National Technical Information Service; 1976. p. 38–54.
- Bird RP, Rohrig N, Colvett RD, Geard CR, Marino SA. Inactivation of synchronized Chinese hamster V79 cells with charged-particle track segments. *Radiat Res* 1980; 82:277–89.
- Jones GDD, Milligan JR, Ward JF, Calabro-Jones PM, Aguilera JA. Yield of strand breaks as a function of scavenger concentration and LET for SV40 irradiated with 4He ions. *Radiat Res* 1993; 136:190–6.
- Kovalchuk O, Zemp F, Filkowski J, Altamirano A, Dickey JS, Jenkins-Baker G, et al. MicroRNAome changes in bystander three-dimensional human tissue models suggest priming of apoptotic pathways. *Carcinogenesis* 2010; 31:1882–8.
- Horowitz YS, Horowitz A, Oster L, Marino S, Datz H, Margaliot M. Investigation of the ionisation density of the glow curve characteristics of  $\text{LiF:Mg,Ti}$ . *Radiat Prot Dosim* 2008; 131:406–13.
- Hei TK, Komatsu K, Hall EJ, Zaider M. Oncogenic transformation by charged particles of defined LET. *Carcinogenesis* 1988; 9:747–50.
- Miller RC, Marino SA, Brenner DJ, Martin SG, Richards M, Randers-Pehrson G, et al. The biological effectiveness of radon-progeny alpha particles. II. Oncogenic transformation as a function of LET. *Radiat Res* 1995; 142:54–60.
- Ghandhi SA, Ming L, Ivanov VN, Hei TK, Amundson SA. Regulation of early signaling and gene expression in the alpha-particle and bystander response of IMR-90 human fibroblasts. *BMC Med Genomics* 2010; 3:31.
- Randers-Pehrson G, Geard CR, Johnson GW, Brenner DJ. The Columbia University single-ion microbeam. *Radiat Res* 2001; 156:210–4.
- Miller RC, Randers-Pehrson G, Geard CR, Hall EJ, Brenner DJ. The oncogenic potential of a single alpha particle. *Proc Natl Acad Sci USA* 1999; 96:19–22.
- Hei TK, Wu LJ, Liu SX, Vannais D, Waldren CA, Randers-Pehrson G. Mutagenic effects of a single and an exact number of  $\alpha$  particles in mammalian cells. *Proc Natl Acad Sci USA* 1997; 94:3765–70.
- Wu LJ, Randers-Pehrson G, Waldren CA, Geard CR, Yu YZ, Hei TK. Biological consequence of cytoplasmic irradiation: role of reactive oxygen species. *Proc Natl Acad Sci USA* 1999; 96:4959–64.
- Zhou H, Randers-Pehrson G, Waldren CA, Vannais D, Hall EJ, Hei TK. Induction of a bystander mutagenic effect of alpha particles in mammalian cells. *Proc Natl Acad Sci USA* 2000; 97:2099–104.
- Dymnikov AD, Brenner DJ, Johnson G, Randers-Pehrson G. Theoretical study of short electrostatic lens for the Columbia ion microprobe. *Rev Sci Instr* 2000; 71:1646–50.
- Randers-Pehrson G, Johnson GW, Marino SA, Xu Y, Dymnikov

- AD, Brenner DJ. The Columbia University sub-micron charged particle beam. *Nucl Instr Meth A* 2009; 609:294–9.
30. Zhou H, Ivanov VN, Gillespie J, Geard CR, Amundson SA, Brenner DJ, et al. Mechanism of radiation-induced bystander effect: Role of the cyclooxygenase-2 signaling pathway. *Proc Nat Acad Sci USA* 2005; 102:14641–6.
  31. Belyakov OV, Mitchell SA, Parikh D, Randers-Pehrson G, Marino SA, Amundson SA, et al. Biological effects in unirradiated human tissue as a response to radiation damage up to 1 mm away. *Proc Nat Acad Sci USA* 2005; 102:14203–8.
  32. Bertucci A, Pocock R, Randers-Pehrson G, Brenner DJ. Microbeam irradiation of the *C. elegans* nematode. *J Radiat Res* 2009; 50:A49–A54.
  33. Buonanno M, Randers-Pehrson G, Smilenov LB, Kleiman NJ, Young E, Ponnayia B, et al. A mouse ear model for bystander studies induced by microbeam irradiation. *Radiat Res* 2015; 184:219–25.
  34. Garty G, Ross GJ, Bigelow A, Randers-Pehrson G, Brenner DJ. A microbeam irradiator without an accelerator. *Nucl Instrum Meth B* 2005; 241:392–6.
  35. Garty G, Ross GJ, Bigelow AW, Randers-Pehrson G, Brenner DJ. Testing the stand-alone microbeam at Columbia University. *Radiat Prot Dos* 2006; 122:292–6.
  36. Garty G, Grad M, Jones BK, Xu Y, Randers-Pehrson G, Attinger D, Brenner DJ. Design of a novel flow-and shoot (FAST) microbeam. *Radiat Prot Dosim* 2011; 143:344–8.
  37. Harken AD, Randers-Pehrson G, Johnson GW, Brenner DJ. The Columbia University proton-induced soft x-ray microbeam. *Nucl Inst Meth B* 2011; 269:1992–6.
  38. Bigelow AW, Geard CR, Randers-Pehrson G, Brenner DJ. Microbeam-integrated multiphoton imaging system. *Rev Sci Instrum* 2008; 79:123707.
  39. Bigelow AW, Ponnaiya B, Targoff K, Brenner DJ. UV microspot irradiator at Columbia University. *Radiat Environ Biophys* 2013; 52:411–7.
  40. Xu Y, Randers-Pehrson G, Marino SA, Bigelow AW, Akselrod MS, Sykora JG, et al. An accelerator-based neutron microbeam system for studies of radiation effects. *Radiat Prot Dosim* 2011; 145:373–6.
  41. Xu Y, Randers-Pehrson G, Turner HC, Marino SA, Geard CR, Brenner DJ, et al. Accelerator-based biological irradiation facility simulating neutron exposure from an improvised nuclear device. *Radiat Res* 2015; 184:404–10.
  42. Brenner DJ, Vazquez M, Buonanno M, Amundson SA, Bigelow AW, Garty G, et al. Integrated interdisciplinary training in the radiological sciences. *Br J Radiol* 2014; 87:20130779.